Acta Crystallographica Section A
Foundations of Crystallography
ISSN 0108-7673

Received 24 November 2002
Accepted 4 March 2003

X-ray Takagi–Taupin dynamical theory generalized to *n*-beam diffraction cases

Kouhei Okitsu

Engineering Research Institute, School of Engineering, The University of Tokyo, Yayoi, Bunkyo-ku, Tokyo 113-8656, Japan. Correspondence e-mail: okitsu@soyak.t.u-tokyo.ac.jp

A new X-ray dynamical diffraction theory that can deal with *n*-beam cases comprehensively ($n \in \{3, 4, 6, 8, 12\}$) has been derived based on the Takagi–Taupin dynamical theory. The new theory takes into account correctly the effects of arbitrarily polarized incident X-rays and the polarization states of X-ray wavefields in a crystal. Furthermore, an arbitrary lattice displacement in the crystal can be dealt with. The new theory has a high symmetry and therefore can be written with one equation supposing that suffixes are taken in $2n$ ways, where the suffixes indicate ordinal numbers of waves and polarization states. This simplicity of the theory enables a computer program to solve the equations to be coded easily. A method to solve the theory numerically is also described. 'Six-beam X-ray section topographs' computer simulated based on the new theory are also presented.

1. Introduction

After Laue's great work in 1912, Darwin (1914*a*,*b*), Ewald (1917) and Laue (1931) constructed the X-ray dynamical diffraction theories. Since the late 1950's when the technologies to grow almost perfect silicon crystals were developed, the two-beam X-ray dynamical diffraction theories and related physics have attained significant growth to date as is reviewed *e.g.* by Authier & Malgrange (1998) and Authier (2001). Nowadays, the widespread theory called the Ewald–Laue theory (Laue, 1931) is regarded as the general two-beam X-ray dynamical diffraction theory for a perfect crystal. Among a great quantity of theoretical works, however, a theory derived by Takagi (1962, 1969) and Taupin (1964) is worthy of special mention. In this theory, wavefields of X-rays in a crystal are represented by partial differential equations in the real space of the crystal. The Takagi–Taupin equations can deal with X-ray wavefields in an arbitrarily distorted crystal. The approximation used when deriving the Takagi–Taupin equations is excellent so that X-ray wavefields in crystals with practically all kinds of defects can be described (Härtwig, 2001). Based on the Takagi–Taupin equations, Kato (1976*a*,*b*, 1979, 1980*a*,*b*,*c*) presented a theory that can deal with X-ray wavefields in a crystal including random lattice distortion using a statistical procedure for the purpose that dynamical diffraction phenomena in a mosaic crystal can be discussed.

On the other hand, since the early age of X-ray diffraction physics, X-ray multibeam diffraction (Wagner, 1920; Berg, 1926; Schachenmeier, 1923; Cauchois *et al.*, 1937), in which more than two waves are strong in a crystal, has attracted much attention for a long time. Several authors extended the Ewald–Laue two-beam dynamical theory to multibeam diffraction (simultaneous reflection) cases (Mayer, 1928; Weigle & Mühsam, 1937; Blanc & Weigle, 1937; Renninger, 1937; Ewald & Héno, 1968). Such phenomena as *Aufhellung* and *Umweganregung* owing to the X-ray multibeam diffraction cases were qualitatively explained in the above works. However, the multibeam diffraction dynamical theories mentioned above are still difficult even for recent scientists to solve the equations. This situation is mainly due to the difficulty in dealing with the effects of polarization of X-ray wavefields.

Incidentally, Ott (1938), Bijvoet & MacGillavry (1939) and Lipscomb (1949) pointed out for the first time, independently, that X-ray intensity profiles in the vicinity of a three-beam diffraction case depend on the structure-factor phase (triplet phase invariant). Since an experimental work was published by Colella (1974), this candidate for a method to solve the phase problem in X-ray crystal structure analysis has come to be recognized by several authors (Post, 1977, 1979; Shen, 1986; Chang, 1986; Weckert *et al.*, 1993) and is in progress even at the present time (Weckert & Hümmer, 1997, 1998; Thorkildsen & Larsen, 1998; Larsen & Thorkildsen, 1998; Stetsko *et al.*, 2001). While the dependence of structure-factor phases on the X-ray intensity profiles when the multibeam diffraction occurs is a dynamical diffraction effect, real crystals whose structures have to be analyzed are mosaic crystals but not perfect enough to be dealt with directly by the dynamical theory. Therefore, if Kato's procedure to deal with the random lattice distortion is applied to a Takagi–Taupin-type dynamical theory extended to the cases of multibeam reflection, the derived theory may be able to deal with the correlation between the multibeam X-ray diffraction profile and the phase problem of mosaic crystals, as is pointed out by Thorkildsen

(1987), Thorkildsen & Larsen (1998), Larsen & Thorkildsen (1998) and Thorkildsen *et al.* (2001). The above authors solved a Takagi–Taupin-type dynamical theory extended to the three-beam case in which, however, the effects of polarization are neglected (Thorkildsen, 1987). This situation related to the multibeam cases and the phase problem has been reviewed by Authier (2001).

As is well known, electromagnetic waves have the features of polarization since the wave equation derived from the Maxwell equations with a condition that $\mathrm{div}\,\mathbf{D}(\mathbf{r}) = 0$ reveals the transversality of electromagnetic waves, where $\mathbf{D}(\mathbf{r})$ is the oscillatory component of the electric displacement vector. As described by Takagi (1969), his fundamental equation of dynamical diffraction appearing as equation (6) in the present paper has been considered for 40 years to be extremely difficult to solve in the n-beam cases, owing to the transversality of X-rays. In the present paper, a new theory based on the Takagi–Taupin dynamical theory is described, which can deal with the n-beam case ($n \in \{3, 4, 6, 8, 12\}$) dynamical diffraction comprehensively in a crystal including arbitrary lattice displacements, without neglecting the effect of polarization. The new theory can be written with a partial differential equation whose suffixes are taken in $2n$ ways. The high symmetry of the equation enabled the present author to code a computer program to solve the new theory numerically.

2. Derivation of theory

2.1. Definition of '*n*-beam cases'

First, let us specify the number n in the 'n-beam' dynamical diffraction theory discussed in the present paper. Fig. 1 shows schematically a condition in the three-dimensional reciprocal space in which the three-beam diffraction condition is satisfied. Fig. 1 also shows $N_o^{(1)}$ (rectangle $PQB_o^{(1)}A_o^{(1)}$), $N_1^{(2)}$ (rectangle $PQB_1^{(2)}A_1^{(2)}$) and $N_2^{(o)}$ (rectangle $PQB_2^{(o)}A_2^{(o)}$), which are perpendicular bisector planes of line segments H_0H_1, H_1H_2 and H_2H_0, respectively. Here, H_0 is the origin of the reciprocal space. H_1 and H_2 are reciprocal-lattice points. Q is the circumcenter of triangle $H_0H_1H_2$. P is the starting point of X-ray wavevectors $\overrightarrow{PH_0}$, $\overrightarrow{PH_1}$ and $\overrightarrow{PH_2}$ when the simultaneous reflection condition is completely satisfied. These planes $N_o^{(1)}$, $N_1^{(2)}$ and $N_2^{(o)}$ cross with one another at a line PQ which is normal to the plane $H_0H_1H_2$ in Fig. 1. Fig. 2 is a schematic drawing in the three-dimensional real space showing that X-rays transmitted through a pinhole are incident on a crystal in which three wavefields are excited and are propagated in the directions $\overrightarrow{E_oS_o}$ (forward-diffracted beam), $\overrightarrow{E_oS_1}$ and $\overrightarrow{E_oS_2}$. When performing an experiment as shown in Fig. 2, the incident X-rays even somewhat monochromated and collimated should be considered to have nonzero energy spread and angular divergence, that is the starting point of the wavevector in Fig. 1 is considered to be located near P. When the starting point of the wavevector of the incident X-rays (hereafter referred to as P_1) is located in the vicinity of the line PQ, wavefields are excited in a triangular pyramid whose apex is E_o and whose base is the triangle $S_oS_1S_2$ in Fig. 2. Hereafter, this case is referred to as case (A). When P_1 is apart from PQ but is located in the vicinity of the planes $N_o^{(1)}$ or $N_2^{(o)}$ in Fig. 1, the incident X-rays excite wavefields in triangles $E_oS_oS_1$ or $E_oS_2S_o$ in Fig. 2, respectively. Hereafter, these circumstances are referred to as cases (B_1) and (B_2). After diffraction in the crystal, the three wavefields located in the triangle $S_oS_1S_2$ in Fig. 2 propagate in the directions of $\overrightarrow{E_oS_o}$, $\overrightarrow{E_oS_1}$ and $\overrightarrow{E_oS_2}$ and follow separate paths. They are recorded on a two-dimensional X-ray detector. X-ray intensity photographs of three-beam cases [case (A)] are recorded on planar areas inside triangles $S_o'S_1'S_2'(\overrightarrow{E_oS_o})$, $S_o'S_1'S_2'(\overrightarrow{E_oS_1})$ and $S_o'S_1'S_2'(\overrightarrow{E_oS_2})$, which are projections of $S_oS_1S_2$ on the two-dimensional detector in the directions of $\overrightarrow{E_oS_o}$, $\overrightarrow{E_oS_1}$ and $\overrightarrow{E_oS_2}$, respectively. Hereafter, $X'(\overrightarrow{E_oS_i})$ means projection of X on the two-dimensional detector in the direction of $\overrightarrow{E_oS_i}$, where X is a line segment or a point. The two-beam X-ray intensities corresponding to the reflection vector $\overrightarrow{H_0H_1}$ only [case (B_1)] are recorded on edge lines $S_o'S_1'(\overrightarrow{E_oS_o})$ and $S_o'S_1'(\overrightarrow{E_oS_1})$. X-ray intensities by only $\overrightarrow{H_0H_2}$ [case (B_2)] are recorded on edge lines $S_o'S_2'(\overrightarrow{E_oS_o})$ and $S_o'S_2'(\overrightarrow{E_oS_2})$. When P_1 is located away from the planes $N_o^{(1)}$ or $N_2^{(o)}$ in Fig. 1, diffraction does not occur and X-rays just

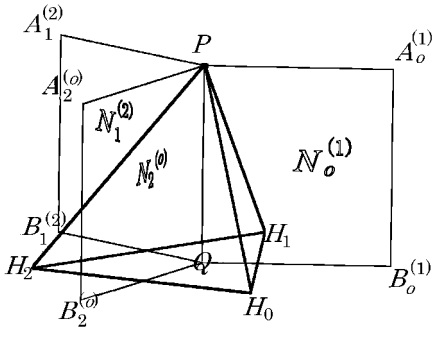

Figure 1
A schematic drawing in the reciprocal space showing that an incident X-ray beam whose wavevector is $\overrightarrow{PH_0}$ is simultaneously reflected by reflection vectors $\overrightarrow{H_0H_1}$ and $\overrightarrow{H_0H_2}$.

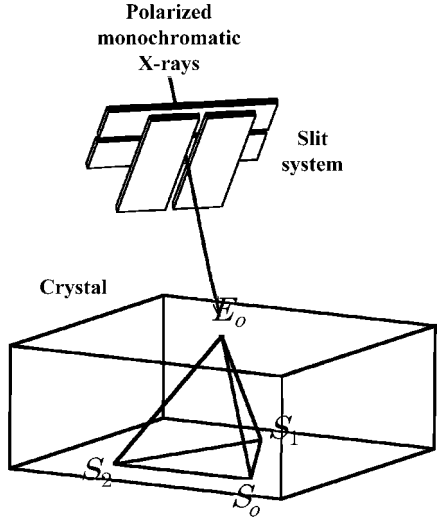

Figure 2
A schematic drawing in the real space showing a 'three-beam X-ray section topography' experiment. An X-ray beam completely polarized in an arbitrary polarization state is incident on a crystal at point E_o.

absorbed in the crystal give the transmitted X-ray intensity at a point $S'_o(\overrightarrow{E_oS_o})$. This case is hereafter referred to as case (C). When P_1 has a somewhat broad distribution, cases (A), (B) and (C) can occur simultaneously. What is important is that the X-ray intensities due to cases (A), (B) and (C) can be observed separately on the two-dimensional detector. In the experiment as shown in Fig. 2, a planar intensity profile due to case (A) can be observed separately from cases (B) and (C). In the present paper, equations describing case (A) are derived, the results calculated from which can be compared with the results of the experiment as shown in Fig. 2.

Fig. 3 shows schematically a four-beam case in the reciprocal space. H_0 is the origin of the reciprocal space. H_1, H_2 and H_3 are reciprocal-lattice points. $H_0H_1H_2H_3$ is a rectangle whose center is Q. Line PQ is normal to the plane of $H_0H_1H_2H_3$. Similarly to the case of Fig. 1, when the starting point of the wavevector of the incident X-rays, P_1 is located in the vicinity of line PQ, the simultaneous diffraction case in which four waves are simultaneously strong in the crystal [case (A)] can occur. On the other hand, Fig. 4 shows schematically a situation where a reciprocal point H'_3 is on an Ewald sphere by chance at a particular photon energy in the condition that H_0, H_1 and H_2 are on the Ewald sphere. $H_0H_1H_2H'_3$ is not a rectangle. In the present paper, this case is not dealt with as a four-beam case. In this case, since line PQ as shown in Fig. 3 cannot be defined for $H_0H_1H_2H'_3$, which is not coplanar, three-beam cases due to triangles in the reciprocal space $H_0H_1H_2$, $H_0H_2H'_3$ and $H_0H'_3H_1$ are considered to occur independently. In a cubic crystal, the n-beam cases for which line PQ as shown in Figs. 1 and 3 exists for the n reciprocal-lattice points (including the origin H_0) are cases of $n \in \{3, 4, 6, 8, 12\}$. The number n was discussed by Burbank (1965) for any crystal system. These cases in which case (A) can occur for the n reciprocal-lattice points are discussed comprehensively in the present paper.

2.2. Definition of the Laue and Lorentz points for an n-beam case

Now, the Laue and Lorentz points have to be defined for later discussion. In this paper, the Laue point La whose location vector is **La** is defined to be a point whose distance from the reciprocal-lattice points $H_0, H_1, \ldots, H_{n-1}$ is the common real value K. H_0 is the origin of the reciprocal space. The position vector of H_i is $\mathbf{H}_i$, where $i \in \{0, 1, \ldots, n-1\}$. $K = 1/\lambda$ is the wavenumber of the incident X-ray beam in vacuum. The Lorentz point Lo whose position vector is **Lo** is defined to be a point whose distance from points $H_0, H_1, \ldots, H_{n-1}$ is the identical value $|K(1 + \frac{1}{2}\chi_o)|$, where χ_o is the zeroth-order Fourier component of electric susceptibility in the crystal. Let us now more clearly define the Lorentz point Lo using the points $H_0, H_1, \ldots, H_{n-1}$, P and Q. The angles $\angle QPH_i$ obviously have the same value, which is hereafter referred to as $\Theta_B^{(\mathrm{Max})}$. Here, let us define a complex vector $\overrightarrow{LaLo} = \Delta\mathbf{k}$ as follows:

$$\overrightarrow{LaLo} = \Delta\mathbf{k} \tag{1}$$

$$= -\tfrac{1}{2}\chi_o K\left[\overrightarrow{PQ}\Big/|\overrightarrow{PQ}|\cos\Theta_B^{(\mathrm{Max})}\right] \tag{2}$$

$$= (1 - n_o)K\left[\overrightarrow{PQ}\Big/|\overrightarrow{PQ}|\cos\Theta_B^{(\mathrm{Max})}\right]. \tag{3}$$

Here, n_o is the refractive index of the crystal. Therefore, the Lorentz point Lo is defined as follows:

$$\mathbf{Lo} = \mathbf{La} + \overrightarrow{LaLo} \tag{4}$$

$$= \mathbf{La} - \tfrac{1}{2}\chi_o K\left[\overrightarrow{PQ}\Big/|\overrightarrow{PQ}|\cos\Theta_B^{(\mathrm{Max})}\right]. \tag{5}$$

2.3. Notations used in Takagi's article and the present paper

The notations used in Takagi's article (Takagi, 1969) are changed for convenience in the present paper according to Table 1 which summarizes the notations used in Takagi (1969) and in the present paper. The meaning of these notations will be explained when they appear for the first time.

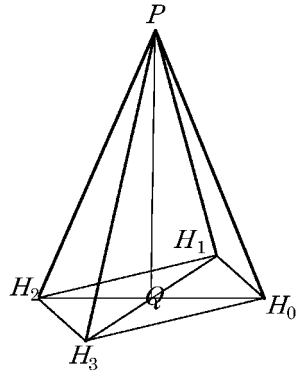

Figure 3
A schematic drawing in the reciprocal space showing that a four-beam simultaneous diffraction condition is satisfied. Vector $\overrightarrow{PH_0}$ is the wavevector of the incident X-rays. Vector $\overrightarrow{PH_1}$, $\overrightarrow{PH_2}$ and $\overrightarrow{PH_3}$ are wavevectors of the simultaneously diffracted X-rays. When the 'n-beam case' discussed in the present paper is satisfied, $H_0, H_1, \ldots, H_{n-1}$ have to be coplanar.

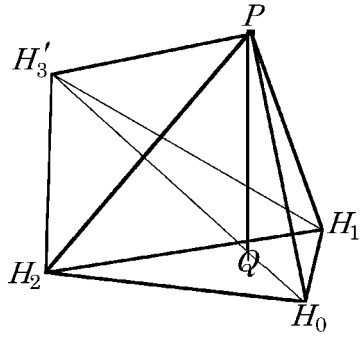

Figure 4
A schematic drawing showing that H_0, H_1, H_2, H'_3 are located on an Ewald sphere whose center is P. This case is not discussed as a 'four-beam case' in the present paper.

Table 1
Notations in Takagi's article (Takagi, 1969) are changed according to this table for convenience for discussions in the present paper.

Notations $\mathbf{g}$, $\sum_g$, $\mathbf{D}'_g$ and $\mathbf{k}_g$ are distinguished from $\mathbf{h}$, $\sum_h$, $\mathbf{D}'_h$ and $\mathbf{k}_h$ in Takagi (1969). However, since $\mathbf{g}$, $\sum_g$, $\mathbf{D}'_g$ and $\mathbf{k}_g$ turn out to be the same as $\mathbf{h}$, $\sum_h$, $\mathbf{D}'_h$ and $\mathbf{k}_h$ after integration with respect to $\mathbf{r}$ over a unit cell, the table does not summarize notations including '$\mathbf{g}$'. $\mathbf{D}'_i(\mathbf{r})$, $[\mathbf{D}'_j(\mathbf{r})]_{\mathbf{s}_i}$ and $\beta'_i(\mathbf{r})$ specify explicitly that these parameters are functions of the position vector $\mathbf{r}$.

Notations in Takagi (1969)	Notations in the present paper	Type of notation	[Dimension]
$\mathbf{D}'_h$	$\mathbf{D}'_i(\mathbf{r})$	Complex vector	[A s m^{-2}]
$[\mathbf{D}'_{h'}]_h$	$[\mathbf{D}'_j(\mathbf{r})]_{\mathbf{s}_i}$	Complex vector	[A s m^{-2}]
$\mathbf{h}$	$\mathbf{h}_i$	Real vector	[m^{-1}]
$\mathbf{h}'$	$\mathbf{h}_j$	Real vector	[m^{-1}]
$\mathbf{k}_h$	$\mathbf{k}_i$	Complex vector	[m^{-1}]
$\mathbf{K}_h$	$\mathbf{K}_i$	Real vector	[m^{-1}]
$\partial/\partial s_h$	$\partial/\partial s_i$	Differentiation in the real space	[m^{-1}]
$\mathbf{s}_h$	$\mathbf{s}_i$	Real unit vector	[No dimension]
β_h	β_i	Complex scalar	[No dimension]
β'_h	$\beta'_i(\mathbf{r})$	Complex scalar	[No dimension]
$\chi_{h-h'}$	$\chi_{h_i-h_j}$	Complex scalar	[No dimension]

2.4. Transformation of Takagi's fundamental equation of dynamical diffraction

Equation (39) in Takagi's article (Takagi, 1969) describes the fundamental equation of X-ray diffraction in a distorted crystal as follows:

$$(\mathbf{s}_i \cdot \mathrm{grad})\mathbf{D}'_i(\mathbf{r}) = \mathrm{i}2\pi K\beta'_i(\mathbf{r})\mathbf{D}'_i(\mathbf{r}) - \mathrm{i}\pi K \sum_{j\neq i} \chi_{h_i-h_j}\left[\mathbf{D}'_j(\mathbf{r})\right]_{\mathbf{s}_i}. \quad (6)$$

Here, $\mathbf{s}_i$ is a unit vector in the direction of $\mathbf{K}_i = \mathbf{K}_0 + \mathbf{h}_i$, where $\mathbf{K}_0$ and $\mathbf{h}_i$ are the wavevector of incident X-rays in a vacuum and a reciprocal-lattice vector, respectively. $\mathbf{D}'_i(\mathbf{r})$ is a complex electric displacement vector whose wavevector in the crystal is $\mathbf{K}_i - \Delta\mathbf{k} - \mathrm{grad}[\mathbf{h}_i \cdot \mathbf{u}(\mathbf{r})]$. $\chi_{h_i-h_j}$ is the $(\mathbf{h}_i - \mathbf{h}_j)$-order Fourier component of electric susceptibility in the crystal. $[\mathbf{D}'_j(\mathbf{r})]_{\mathbf{s}_i}$ is a vector component of $\mathbf{D}'_j(\mathbf{r})$ perpendicular to $\mathbf{s}_i$, that is

$$[\mathbf{D}'_j(\mathbf{r})]_{\mathbf{s}_i} = -\mathbf{s}_i \times [\mathbf{s}_i \times \mathbf{D}'_j(\mathbf{r})].$$

$\beta'_i(\mathbf{r})$ is given by

$$\beta'_i(\mathbf{r}) = \beta_i - (1/K)\partial[\mathbf{h}_i \cdot \mathbf{u}(\mathbf{r})]/\partial s_i. \quad (7)$$

Here, $\mathbf{u}(\mathbf{r})$ is a lattice displacement vector. Parameter β_i was defined by Takagi (1969) and represents the angular deviation of the incident X-ray beam from the strict Bragg condition. However, even if β_i is fixed at zero for mathematical convenience, the generality of the fundamental equation (6) does not collapse. Then,

$$\beta'_i(\mathbf{r}) = -(1/K)\partial[\mathbf{h}_i \cdot \mathbf{u}(\mathbf{r})]/\partial s_i, \quad \text{where} \quad \beta_i = 0.$$

Appendix *A* describes that the final form of the present theory (39) derived under the condition that β_i is zero can be solved even when plane-wave X-rays whose wavevector deviates from $\overrightarrow{LaH_0}$ are incident on a crystal. Now, we can rewrite (6) as follows:

$$(\mathbf{s}_i \cdot \mathrm{grad})\mathbf{D}'_i(\mathbf{r}) = -\mathrm{i}2\pi\{\partial[\mathbf{h}_i \cdot \mathbf{u}(\mathbf{r})]/\partial s_i\}\mathbf{D}'_i(\mathbf{r}) - \mathrm{i}\pi K \sum_{j\neq i} \chi_{h_i-h_j}[\mathbf{D}'_j(\mathbf{r})]_{\mathbf{s}_i}. \quad (8)$$

On the other hand, the whole electric displacement vector in the crystal $\mathbf{D}(\mathbf{r})$ is defined by equation (30) in Takagi's article (Takagi, 1969) as follows:

$$\mathbf{D}(\mathbf{r}) = \sum_g \mathbf{D}'_g(\mathbf{r}) \exp\{-\mathrm{i}2\pi[\mathbf{k}_g \cdot \mathbf{r} - \mathbf{g} \cdot \mathbf{u}(\mathbf{r})]\}.$$

In Takagi's article, $\sum_g$, $\mathbf{D}'_g$, $\mathbf{k}_g$ and $\mathbf{g}$ are distinguished from $\sum_h$, $\mathbf{D}'_h$, $\mathbf{k}_h$ and $\mathbf{h}$. However, after integration with respect to $\mathbf{r}$ over a unit cell, the above equation turns out to be the same as an equation using $\mathbf{h}$ in place of $\mathbf{g}$. Therefore, according to Table 1, we obtain

$$\mathbf{D}(\mathbf{r}) = \sum_i \mathbf{D}'_i(\mathbf{r}) \exp\{-\mathrm{i}2\pi[\mathbf{k}_i \cdot \mathbf{r} - \mathbf{h}_i \cdot \mathbf{u}(\mathbf{r})]\}. \quad (9)$$

Here, $\mathbf{k}_i$ is $\overrightarrow{LoH_i}$ $(= \mathbf{K}_i - \Delta\mathbf{k})$. The above equation (9) can be transformed to

$$\mathbf{D}(\mathbf{r}) = \sum_i \mathbf{D}_i(\mathbf{r}) \exp(-\mathrm{i}2\pi\mathbf{k}_i \cdot \mathbf{r}), \quad (10)$$

where

$$\mathbf{D}_i(\mathbf{r}) = \mathbf{D}'_i(\mathbf{r}) \exp[+\mathrm{i}2\pi\mathbf{h}_i \cdot \mathbf{u}(\mathbf{r})]. \quad (11)$$

Substituting *i* by *j*, we get

$$\mathbf{D}_j(\mathbf{r}) = \mathbf{D}'_j(\mathbf{r}) \exp[+\mathrm{i}2\pi\mathbf{h}_j \cdot \mathbf{u}(\mathbf{r})]. \quad (12)$$

Substituting (11) and (12) into (8), we obtain

$$\begin{aligned}(\mathbf{s}_i \cdot \mathrm{grad})\{\mathbf{D}_i(\mathbf{r}) &\exp[-\mathrm{i}2\pi\mathbf{h}_i \cdot \mathbf{u}(\mathbf{r})]\} \\ &= -\mathrm{i}2\pi\{\partial[\mathbf{h}_i \cdot \mathbf{u}(\mathbf{r})]/\partial s_i\}\mathbf{D}_i(\mathbf{r}) \exp[-\mathrm{i}2\pi\mathbf{h}_i \cdot \mathbf{u}(\mathbf{r})] \\ &\quad - \mathrm{i}\pi K \sum_{j\neq i} \chi_{h_i-h_j}[\mathbf{D}_j(\mathbf{r})]_{\mathbf{s}_i} \exp[-\mathrm{i}2\pi\mathbf{h}_j \cdot \mathbf{u}(\mathbf{r})]. \quad (13)\end{aligned}$$

The left-hand side of (13) is transformed to

$$\begin{aligned}(\mathbf{s}_i \cdot \mathrm{grad})\{\mathbf{D}_i(\mathbf{r}) &\exp[-\mathrm{i}2\pi\mathbf{h}_i \cdot \mathbf{u}(\mathbf{r})]\} \\ &= [(\mathbf{s}_i \cdot \mathrm{grad})\mathbf{D}_i(\mathbf{r})] \exp[-\mathrm{i}2\pi\mathbf{h}_i \cdot \mathbf{u}(\mathbf{r})] \\ &\quad + \mathbf{D}_i(\mathbf{r})\{\partial[\mathbf{h}_i \cdot \mathbf{u}(\mathbf{r})]/\partial s_i\}(-\mathrm{i}2\pi) \exp[-\mathrm{i}2\pi\mathbf{h}_i \cdot \mathbf{u}(\mathbf{r})]. \quad (14)\end{aligned}$$

Substituting (14) into the left-hand side of (13), we obtain

$$\begin{aligned}(\mathbf{s}_i \cdot \mathrm{grad})&\mathbf{D}_i(\mathbf{r}) \\ &= -\mathrm{i}\pi K \sum_{j\neq i} \chi_{h_i-h_j} \exp[-\mathrm{i}2\pi(\mathbf{h}_j - \mathbf{h}_i) \cdot \mathbf{u}(\mathbf{r})][\mathbf{D}_j(\mathbf{r})]_{\mathbf{s}_i}. \quad (15)\end{aligned}$$

Equation (15) is a form of the fundamental equation of X-ray dynamical diffraction theory, based on which final equations (25) and (39) will be derived in §§2.5 and 2.6.

2.5. Scalar expansion of the fundamental equation and definition of polarization factors

In order to solve (15), the vectors $\mathbf{D}_i(\mathbf{r})$ and $\mathbf{D}_j(\mathbf{r})$ must be decomposed with respect to a set of unit vectors. For example, let us consider a hexagonal pyramid as shown in Fig. 5. The direction of unit vector $\mathbf{s}_i$ is parallel to $\mathbf{K}_i$. Another set of vectors, $\mathbf{e}_i$ and $\mathbf{e}_{(i+1)'}$ is defined as follows:

$$\mathbf{e}_i = \frac{\mathbf{s}_{(i-1)'} \times \mathbf{s}_i}{|\mathbf{s}_{(i-1)'} \times \mathbf{s}_i|}, \quad \mathbf{e}_{(i+1)'} = \frac{\mathbf{s}_i \times \mathbf{s}_{(i+1)'}}{|\mathbf{s}_i \times \mathbf{s}_{(i+1)'}|},$$

where $(i-1)'$ and $(i+1)'$ are $\mathrm{mod}(i-1, n)$ and $\mathrm{mod}(i+1, n)$, respectively, that is the remainder of $(i-1)$ and $(i+1)$ when divided by n. Therefore, when $i = 0$, $(i-1)'$ is $n-1$. When $i = n-1$, $(i+1)'$ is zero. Evidently, $\mathbf{e}_i$ is perpendicular to $\mathbf{s}_i$ and $\mathbf{s}_{(i-1)'}$. In order to derive scalar equations equivalent to the fundamental equation (15), $\mathbf{D}_i$ and $\mathbf{D}_j$ are written as follows:

$$\mathbf{D}_i(\mathbf{r}) = D_i^{(0)}(\mathbf{r})\mathbf{e}_i + D_i^{(1)}(\mathbf{r})\mathbf{e}_{(i+1)'}, \tag{16}$$

$$\mathbf{D}_j(\mathbf{r}) = D_j^{(0)}(\mathbf{r})\mathbf{e}_j + D_j^{(1)}(\mathbf{r})\mathbf{e}_{(j+1)'}. \tag{17}$$

Here, $D_i^{(0)}(\mathbf{r})$, $D_i^{(1)}(\mathbf{r})$, $D_j^{(0)}(\mathbf{r})$ and $D_j^{(1)}(\mathbf{r})$ are scalar values of the electric displacement. Appendix *B* validates that the electric displacement vectors can be expanded in a combination of scalar components whose unit vectors cross obliquely. Substituting (16) and (17) into (15), we obtain

$$\begin{aligned}(\mathbf{s}_i \cdot \mathrm{grad})[D_i^{(0)}(\mathbf{r})\mathbf{e}_i + D_i^{(1)}(\mathbf{r})\mathbf{e}_{(i+1)'}] \\ = -\mathrm{i}\pi K \sum_{j\neq i}\{\chi_{h_i-h_j} \exp[-\mathrm{i}2\pi(\mathbf{h}_j - \mathbf{h}_i)\cdot\mathbf{u}(\mathbf{r})] \\ \times [D_j^{(0)}(\mathbf{r})\mathbf{e}_j + D_j^{(1)}(\mathbf{r})\mathbf{e}_{(j+1)'}]_{\mathbf{s}_i}\}.\end{aligned} \tag{18}$$

Here, let us introduce a coordinate system with unit vectors $\mathbf{s}_i$, $\mathbf{e}_i^{(\sigma)}$ and $\mathbf{e}_i^{(\pi)}$ which construct an orthogonal right-handed system in this order. $\mathbf{e}_i^{(\sigma)}$ is perpendicular to $\overrightarrow{PQ}$ in Fig. 1 and to $\mathbf{s}_i$, then strictly defined by

$$\mathbf{e}_i^{(\sigma)} = \frac{\mathbf{s}_i \times \overrightarrow{PQ}}{|\mathbf{s}_i \times \overrightarrow{PQ}|}, \tag{19}$$

and $\mathbf{e}_i^{(\pi)}$ is defined by

$$\mathbf{e}_i^{(\pi)} = \mathbf{s}_i \times \mathbf{e}_i^{(\sigma)}. \tag{20}$$

Geometrical relations among $\mathbf{s}_i$, $\mathbf{e}_i$, $\mathbf{e}_{(i+1)'}$, $\mathbf{e}_i^{(\sigma)}$ and $\mathbf{e}_i^{(\pi)}$ are shown in Fig. 6. The operator grad is given by using the $\mathbf{s}_i$–$\mathbf{e}_i^{(\sigma)}$–$\mathbf{e}_i^{(\pi)}$ orthogonal coordinate system as follows:

$$\mathrm{grad} = \frac{\partial}{\partial s_i}\mathbf{s}_i + \frac{\partial}{\partial e_i^{(\sigma)}}\mathbf{e}_i^{(\sigma)} + \frac{\partial}{\partial e_i^{(\pi)}}\mathbf{e}_i^{(\pi)}.$$

Here, s_i, $e_i^{(\sigma)}$ and $e_i^{(\pi)}$ are coordinate values of the position vector $\mathbf{r}$ in the real space. Therefore, $\mathbf{r}$ is represented by a combination of $\mathbf{s}_i$, $\mathbf{e}_i^{(\sigma)}$ and $\mathbf{e}_i^{(\pi)}$ as follows:

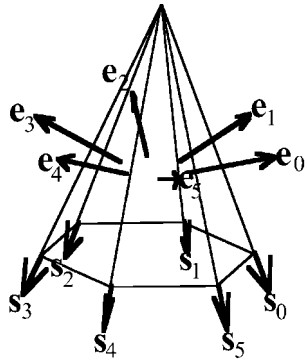

Figure 5
Sets of unit vectors $\mathbf{s}_i$ and $\mathbf{e}_i$ where $i \in \{0, 1, \ldots, n-1\}$. Here, $n = 6$.

$$\mathbf{r} = s_i\mathbf{s}_i + e_i^{(\sigma)}\mathbf{e}_i^{(\sigma)} + e_i^{(\pi)}\mathbf{e}_i^{(\pi)}. \tag{21}$$

Then, the operator $\mathbf{s}_i \cdot \mathrm{grad}$ is represented as follows:

$$\mathbf{s}_i \cdot \mathrm{grad} = \mathbf{s}_i \cdot \left(\frac{\partial}{\partial s_i}\mathbf{s}_i + \frac{\partial}{\partial e_i^{(\sigma)}}\mathbf{e}_i^{(\sigma)} + \frac{\partial}{\partial e_i^{(\pi)}}\mathbf{e}_i^{(\pi)}\right) = \frac{\partial}{\partial s_i}.$$

Therefore, the left-hand side of (18) is given by

$$\begin{aligned}(\mathbf{s}_i \cdot \mathrm{grad})[D_i^{(0)}(\mathbf{r})\mathbf{e}_i + D_i^{(1)}(\mathbf{r})\mathbf{e}_{(i+1)'}] \\ = \frac{\partial}{\partial s_i}D_i^{(0)}(\mathbf{r})\mathbf{e}_i + \frac{\partial}{\partial s_i}D_i^{(1)}(\mathbf{r})\mathbf{e}_{(i+1)'}.\end{aligned} \tag{22}$$

Here, (22) is considered to be evident. However, Appendix *B* validates (22) by using the $\mathbf{s}_i$–$\mathbf{e}_i^{(\sigma)}$–$\mathbf{e}_i^{(\pi)}$ orthogonal coordinate system. On the other hand, $\mathbf{e}_j$ can be necessarily represented by a combination of $\mathbf{s}_i$, $\mathbf{e}_i$ and $\mathbf{e}_{(i+1)'}$ as follows:

$$\mathbf{e}_j = S^{(j,i)}\mathbf{s}_i + C_0^{(j,i)}\mathbf{e}_i + C_1^{(j,i)}\mathbf{e}_{(i+1)'}. \tag{23}$$

$C_0^{(j,i)}$ and $C_1^{(j,i)}$ will turn out to be polarization factors in later discussion. Then, $[D_j^{(0)}(\mathbf{r})\mathbf{e}_j + D_j^{(1)}(\mathbf{r})\mathbf{e}_{(j+1)'}]_{\mathbf{s}_i}$ is given by

$$\begin{aligned}[D_j^{(0)}(\mathbf{r})\mathbf{e}_j + D_j^{(1)}(\mathbf{r})\mathbf{e}_{(j+1)'}]_{\mathbf{s}_i} \\ = [D_j^{(0)}(\mathbf{r})C_0^{(j,i)} + D_j^{(1)}(\mathbf{r})C_0^{[(j+1)',i]}]\mathbf{e}_i \\ + [D_j^{(0)}(\mathbf{r})C_1^{(j,i)} + D_j^{(1)}(\mathbf{r})C_1^{[(j+1)',i]}]\mathbf{e}_{(i+1)'}.\end{aligned} \tag{24}$$

Substituting (22) and (24) into (18), and comparing terms of $\mathbf{e}_i$ and $\mathbf{e}_{(i+1)'}$, respectively, we obtain

$$\begin{aligned}\frac{\partial}{\partial s_i}D_i^{(0)}(\mathbf{r}) = -\mathrm{i}\pi K \sum_{j\neq i}\{\chi_{h_i-h_j}\exp[-\mathrm{i}2\pi(\mathbf{h}_j - \mathbf{h}_i)\cdot\mathbf{u}(\mathbf{r})] \\ \times [C_0^{(j,i)}D_j^{(0)}(\mathbf{r}) + C_0^{[(j+1)',i]}D_j^{(1)}(\mathbf{r})]\}, \\ \frac{\partial}{\partial s_i}D_i^{(1)}(\mathbf{r}) = -\mathrm{i}\pi K \sum_{j\neq i}\{\chi_{h_i-h_j}\exp[-\mathrm{i}2\pi(\mathbf{h}_j - \mathbf{h}_i)\cdot\mathbf{u}(\mathbf{r})] \\ \times [C_1^{(j,i)}D_j^{(0)}(\mathbf{r}) + C_1^{[(j+1)',i]}D_j^{(1)}(\mathbf{r})]\}.\end{aligned}$$

Let l and m be $l, m \in \{0, 1\}$, which represent polarization states of the ith and jth waves, respectively. We obtain

$$\begin{aligned}\frac{\partial}{\partial s_i}D_i^{(l)}(\mathbf{r}) = -\mathrm{i}\pi K \sum_{j\neq i}\sum_{m=0}^{1}\chi_{h_i-h_j}\exp[-\mathrm{i}2\pi(\mathbf{h}_j - \mathbf{h}_i)\cdot\mathbf{u}(\mathbf{r})] \\ \times C_l^{[(j+m)',i]}D_j^{(m)}(\mathbf{r}),\end{aligned} \tag{25}$$

where

$$i, j \in \{0,1, \ldots, n-1\}, \quad l, m \in \{0, 1\}, \quad n \in \{3, 4, 6, 8, 12\}.$$

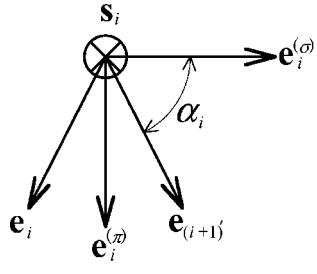

Figure 6
Geometrical relation of the unit vectors $\mathbf{s}_i$, $\mathbf{e}_i$, $\mathbf{e}_{(i+1)'}$, $\mathbf{e}_i^{(\sigma)}$ and $\mathbf{e}_i^{(\pi)}$.

Equation (25) is a final form of the Takagi–Taupin theory extended to n-beam cases. The high symmetry of (25) is achieved by dividing the electric displacement vector $\mathbf{D}_i(\mathbf{r})$ into scalar components whose unit vectors cross obliquely as in (16) and (17). This simplicity of (25) makes it easy to code a computer program numerically to solve the theory.

2.6. Another form of the theory

The new theory derived in §2.5 is written as in (25). Behind this equation, it is assumed that an X-ray wavefield in a crystal $\mathbf{D}(\mathbf{r})$ is represented as in (10). Rewriting (10) with the limitation that $i \in \{0, 1, \ldots, n-1\}$, it follows that

$$\mathbf{D}(\mathbf{r}) = \sum_{i=0}^{n-1} \mathbf{D}_i(\mathbf{r}) \exp(-\mathrm{i}2\pi\mathbf{k}_i \cdot \mathbf{r}). \tag{26}$$

Since the starting point of wavevector $\mathbf{k}_i$ is fixed at the Lorentz point, (26) is transformed to

$$\begin{aligned}\mathbf{D}(\mathbf{r}) &= \sum_{i=0}^{n-1} \mathbf{D}_i(\mathbf{r}) \exp[-\mathrm{i}2\pi(\mathbf{K}_i - \Delta\mathbf{k}) \cdot \mathbf{r}] \\ &= \sum_{i=0}^{n-1} \mathbf{D}_i''(\mathbf{r}) \exp(-\mathrm{i}2\pi\mathbf{K}_i \cdot \mathbf{r}),\end{aligned} \tag{27}$$

where

$$\mathbf{D}_i''(\mathbf{r}) = \mathbf{D}_i(\mathbf{r}) \exp(+\mathrm{i}2\pi\Delta\mathbf{k} \cdot \mathbf{r}). \tag{28}$$

Now, let us represent $\mathbf{D}_i''(\mathbf{r})$ by a combination of scalar components whose unit vectors are $\mathbf{e}_i$ and $\mathbf{e}_{(i+1)'}$ as follows:

$$\mathbf{D}_i''(\mathbf{r}) = D_i''^{(0)}(\mathbf{r})\mathbf{e}_i + D_i''^{(1)}(\mathbf{r})\mathbf{e}_{(i+1)'}. \tag{29}$$

Here, $D_i''^{(0)}(\mathbf{r})$ and $D_i''^{(1)}(\mathbf{r})$ are scalar values of the electric displacement. Substituting (16) into (28), we get

$$\mathbf{D}_i''(\mathbf{r}) = [D_i^{(0)}(\mathbf{r})\mathbf{e}_i + D_i^{(1)}(\mathbf{r})\mathbf{e}_{(i+1)'}] \exp(+\mathrm{i}2\pi\Delta\mathbf{k} \cdot \mathbf{r}). \tag{30}$$

Comparing (29) and (30), we find

$$D_i^{(l)}(\mathbf{r}) = D_i''^{(l)}(\mathbf{r}) \exp(-\mathrm{i}2\pi\Delta\mathbf{k} \cdot \mathbf{r}), \quad \text{where} \quad l \in \{0, 1\}. \tag{31}$$

Using a similar procedure,

$$D_j^{(m)}(\mathbf{r}) = D_j''^{(m)}(\mathbf{r}) \exp(-\mathrm{i}2\pi\Delta\mathbf{k} \cdot \mathbf{r}), \quad \text{where} \quad m \in \{0, 1\}. \tag{32}$$

Substituting (31) and (32) into (25), we obtain

$$\begin{aligned}&\frac{\partial}{\partial s_i}[D_i''^{(l)}(\mathbf{r}) \exp(-\mathrm{i}2\pi\Delta\mathbf{k} \cdot \mathbf{r})] \\ &= -\mathrm{i}\pi K \sum_{j\neq i} \sum_{m=0}^{1} \{\chi_{h_i-h_j} \exp[-\mathrm{i}2\pi(\mathbf{h}_j - \mathbf{h}_i) \cdot \mathbf{u}(\mathbf{r})] \\ &\quad \times C_l^{[(j+m)',i]} D_j''^{(m)}(\mathbf{r}) \exp(-\mathrm{i}2\pi\Delta\mathbf{k} \cdot \mathbf{r})\}.\end{aligned} \tag{33}$$

On the other hand, referring to Figs. 1 and 6,

$$\overrightarrow{PQ}/|\overrightarrow{PQ}| = (\cos\Theta_B^{(\mathrm{Max})})\mathbf{s}_i - (\sin\Theta_B^{(\mathrm{Max})})\mathbf{e}_i^{(\pi)}. \tag{34}$$

Substituting (34) into (1) and (2), we get

$$\Delta\mathbf{k} = -\tfrac{1}{2}\chi_o K\mathbf{s}_i + [\tan\Theta_B^{(\mathrm{Max})}/2]\chi_o K\mathbf{e}_i^{(\pi)}. \tag{35}$$

$\exp(-2\pi\mathrm{i}\Delta\mathbf{k} \cdot \mathbf{r})$ is calculated from (21) and (35) to be

$$\exp(-2\pi\mathrm{i}\Delta\mathbf{k} \cdot \mathbf{r}) = \exp(+\mathrm{i}\pi\chi_o K s_i - \mathrm{i}\pi\chi_o K \tan\Theta_B^{(\mathrm{Max})} e_i^{(\pi)}).$$

Therefore, the left-hand side of (33) is represented as follows:

$$\begin{aligned}&\frac{\partial}{\partial s_i}[D_i''^{(l)}(\mathbf{r}) \exp(-\mathrm{i}2\pi\Delta\mathbf{k} \cdot \mathbf{r})] \\ &= \left[\frac{\partial}{\partial s_i} D_i''^{(l)}(\mathbf{r})\right] \exp(-\mathrm{i}2\pi\Delta\mathbf{k} \cdot \mathbf{r}) \\ &\quad + D_i''^{(l)}(\mathbf{r})\mathrm{i}\pi\chi_o K \exp(-\mathrm{i}2\pi\Delta\mathbf{k} \cdot \mathbf{r}).\end{aligned} \tag{36}$$

Substituting (36) into the left-hand side of (33) and dividing both sides by $\exp(-\mathrm{i}2\pi\Delta\mathbf{k} \cdot \mathbf{r})$, we obtain

$$\begin{aligned}&\frac{\partial}{\partial s_i} D_i''^{(l)}(\mathbf{r}) + \mathrm{i}\pi\chi_o K D_i''^{(l)}(\mathbf{r}) \\ &= -\mathrm{i}\pi K \sum_{j\neq i} \sum_{m=0}^{1} \chi_{h_i-h_j} \exp[-\mathrm{i}2\pi(\mathbf{h}_j - \mathbf{h}_i) \cdot \mathbf{u}(\mathbf{r})] \\ &\quad \times C_l^{[(j+m)',i]} D_j''^{(m)}(\mathbf{r}).\end{aligned} \tag{37}$$

Here, considering polarization factors according to (23) when $j = i$ and $j = (i+1)'$, we obtain

$$C_0^{(i,i)} = 1, \quad C_1^{(i,i)} = 0$$

and

$$C_0^{[(i+1)',i]} = 0, \quad C_1^{[(i+1)',i]} = 1.$$

Therefore, the second term of the left-hand side of (37) can be written as follows:

$$\begin{aligned}\mathrm{i}\pi\chi_o K D_i''^{(l)}(\mathbf{r}) &= \mathrm{i}\pi\chi_o K[C_l^{(i,i)} D_i''^{(0)}(\mathbf{r}) + C_l^{[(i+1)',i]} D_i''^{(1)}(\mathbf{r})] \\ &= \mathrm{i}\pi\chi_o K \sum_{m=0}^{1} [C_l^{[(i+m)',i]} D_i''^{(m)}(\mathbf{r})].\end{aligned} \tag{38}$$

Substituting (38) into (37), we obtain

$$\begin{aligned}\frac{\partial}{\partial s_i} D_i''^{(l)}(\mathbf{r}) &= -\mathrm{i}\pi K \sum_{j=0}^{n-1} \sum_{m=0}^{1} \chi_{h_i-h_j} \exp[-\mathrm{i}2\pi(\mathbf{h}_j - \mathbf{h}_i) \cdot \mathbf{u}(\mathbf{r})] \\ &\quad \times C_l^{[(j+m)',i]} D_j''^{(m)}(\mathbf{r}),\end{aligned} \tag{39}$$

where

$$i, j \in \{0,1, \ldots, n-1\}, \quad l, m \in \{0, 1\}, \quad n \in \{3, 4, 6, 8, 12\}.$$

Equation (39) is another form of the theory.

3. Methodology for solving the theory

The method described here to solve the equations is fundamentally the same as described in Takagi's article (Takagi, 1962). By using the Takagi–Taupin equations, Balibar & Authier (1967) and Taupin (1967) published important works in which dislocation images in X-ray section topographs were numerically calculated and compared with experimental results. Following these studies, Epelboin (1985, 1987) reviewed simulation works based on Takagi–Taupin equations and dealing with the images on X-ray section topographs of such defects as dislocations and/or stacking faults. X-ray section topograph images of strain centers inside and outside

the Borrmann fan were computer simulated and compared with experimental results by Green *et al.* (1990) and by Okitsu *et al.* (1992), respectively, for the first time.

To solve (39), for example, in a six-beam case, a crystal has to be three-dimensionally divided into hexagonal pyramids sufficiently small compared with the extinction length of the $\mathbf{h}_i$ reflection as shown in Fig. 7. When using (39) but not (25), $|\overrightarrow{R_i^{(0)}R^{(1)}}|$ has to be small compared with $1/(\chi_o K)$, which is the extinction length of the $\mathbf{h}_0$ reflection (forward diffraction). In Fig. 7, $\overrightarrow{R_i^{(0)}R^{(1)}}$ is parallel to the direction of $\mathbf{s}_i$. When (39) is satisfied for the wavefields $D_i''^{(l)}(\mathbf{r})$ ($l \in \{0, 1\}$) in the crystal, the following equation has to be satisfied approximately at Rm_i, which is the middle point between $R_i^{(0)}$ and $R^{(1)}$

$$\frac{D_i''^{(l)}(R^{(1)}) - D_i''^{(l)}(R_i^{(0)})}{|\overrightarrow{R_i^{(0)}R^{(1)}}|} = -\mathrm{i}\pi K \sum_{j=0}^{n-1}\sum_{m=0}^{1}\left\{\chi_{h_i-h_j}\exp[-\mathrm{i}2\pi(\mathbf{h}_j-\mathbf{h}_i)\cdot\mathbf{u}(Rm_i)] \times C_l^{[(j+m)',i]}\,\frac{D_j''^{(m)}(R_i^{(0)}) + D_j''^{(m)}(R^{(1)})}{2}\right\}. \quad (40)$$

Here, $D_i''^{(l)}(R_i^{(0)})$ and $D_i''^{(l)}(R^{(1)})$ are complex electric displacements of X-rays at points $R_i^{(0)}$ and $R^{(1)}$ whose wavevector is $\mathbf{K}_i$ and polarization state is *l*. $\mathbf{u}(Rm_i)$ is the lattice displacement vector at Rm_i. For $2n$ values of the electric displacement to be calculated from $2n^2$ known values, the number of equations written as in (40) is $2n$. The simultaneous linear equations (40) can be solved by using a $2n \times 2n$ matrix calculation. For solving (40) in the case of an '*n*-beam X-ray section topograph' experiment as shown in Fig. 2, a boundary condition can be given so that $D_0''^{(0)}(E_o)$ and $D_0''^{(1)}(E_o)$ are nonzero values only at the incident point E_o in Fig. 2, resulting in $D_i''^{(l)}$ of nonzero values only inside the pyramid whose apex is E_o and base is *n*-angular polygon $S_oS_1 \ldots S_{n-1}$ as shown in Fig. 2. The amplitude ratio and phase difference of $D_0''^{(0)}(E_o)$ and $D_0''^{(1)}(E_o)$ depend on the polarization state of the incident X-rays. The solution of (40), $D_i''^{(0)}(R_e)$ and $D_i''^{(1)}(R_e)$, may be transformed into $D_i''^{(\sigma)}(R_e)$ and $D_i''^{(\pi)}(R_e)$ by using (50) and (51) in Appendix *B*, where R_e is a position in the *n*-angular polygon $S_0S_1 \ldots S_{n-1}$ on the exit surface of the crystal. The intensities and polarization states of outgoing X-rays are obtained from $D_i''^{(\sigma)}(R_e)$ and $D_i''^{(\pi)}(R_e)$.

The electric displacement and polarization state of outgoing X-rays when rotating two-dimensionally a perfect crystal around the Bragg condition with incidence of plane-wave X-rays perfectly polarized can be obtained by Fourier transforming $D_i''^{(\sigma)}(R_e)$ and $D_i''^{(\pi)}(R_e)$ calculated for a perfect crystal. This is a transformation inverse to the procedure which is used when Kato derived the spherical-wave dynamical theory (Kato, 1961*a*,*b*, 1968*a*,*b*). Therefore, the Renninger scans (Renninger, 1937) can also be calculated from Fourier transform of $D_i''^{(\sigma)}(R_e)$ and $D_i''^{(\pi)}(R_e)$, which is applicable to obtaining the phase information of crystal structure factors.

There is an important reason why (39) is obtained in §2.6 by transforming (25). The difference between (39) and (25) is that χ_o is explicitly included in the right-hand side of the equation. By taking advantage of this feature of (39), X-ray wavefields in a complex geometry can be numerically calculated with a simple procedure even if the Laue and Bragg geometries are mixed or some objects whose complex refraction index is $n(\mathbf{r}) = n^{(r)}(\mathbf{r}) + \mathrm{i}n^{(i)}(\mathbf{r})$ exists in the X-ray path. The procedure to deal with such a complex geometry will be discussed in a forthcoming separate paper (Okitsu, 2003).

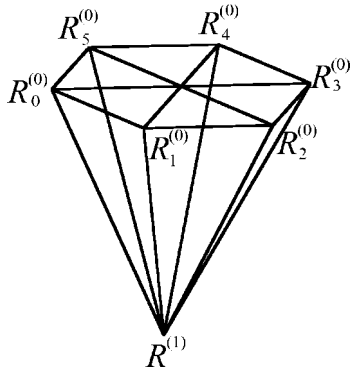

Figure 7
To solve the theory described in (25) or (39), a crystal has to be three-dimensionally divided into sufficiently small wedges. This is a six-beam case.

4. Computer-simulated results based on the new theory

The present author has computer-simulated 'six-beam X-ray section topographs' whose arrangement is assumed as shown in Fig. 8. A $[1\bar{1}1]$-oriented parallel-sided perfect silicon crystal with a thickness of 9.911 mm (which the present author has used in an experiment) was assumed to be adjusted so that 000 (forward diffraction), 440, 484, 088, $\bar{4}48$ and $\bar{4}04$ reflections simultaneously occurred. The X-ray photon energy was

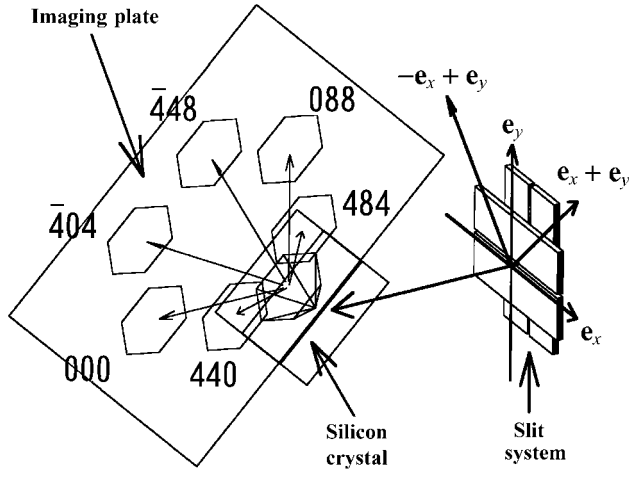

Figure 8
Examples of simulations Figs. 9(*a*) and 9(*b*) were calculated assuming an arrangement shown in this figure. The wavefront of the incident X-rays was assumed to be limited to a sufficiently small size by a slit system. The plane of incidence of the 088 reflection was assumed to be perpendicular to vector $\mathbf{e}_x$ drawn in the figure.

assumed to be 18.5 keV (0.670 Å wavelength and 44.27° Bragg angle for 088 reflection). The crystal was divided into 2000 layers with identical height in the direction of thickness. Every layer was divided into small hexagonal pyramids as shown in Fig. 7. The ridgeline length of the small pyramid corresponding to $|R_i^{(0)}R^{(1)}|$ in (40) was about 6.92 μm. This situation barely satisfied the condition that $|R_i^{(0)}R^{(1)}|$ was sufficiently small compared with $1/(\chi_o K)$ (= 23.7 μm). X-ray wavefields were located in the hexagonal 'Borrmann pyramid' whose apex is the X-ray incident point on the entrance surface of the crystal.

Fig. 9 shows computer-simulated 'six-beam X-ray section topographs' which were expected to appear on an imaging plate shown in Fig. 8. Figs. 9(*a*) and 9(*b*) were obtained under the assumptions of the incident X-rays linearly polarized in the directions of $\mathbf{e}_x + \mathbf{e}_y$ and $-\mathbf{e}_x + \mathbf{e}_y$, respectively, shown in Fig. 8. Bladed patterns are observed approximately perpendicular to the direction of $\mathbf{e}_x + \mathbf{e}_y$ in 000 and $\bar{4}48$ images in Fig. 9(*a*) whereas such patterns are approximately perpendicular to the direction of $-\mathbf{e}_x + \mathbf{e}_y$ in 000 and 484 images in Fig. 9(*b*), which reveals that the polarization effect was probably dealt with correctly in the computer program coded based on (39) and (40). Experimental results in excellent agreement with computer-simulated images will be presented in a forthcoming separate paper (Okitsu *et al.*, 2003).

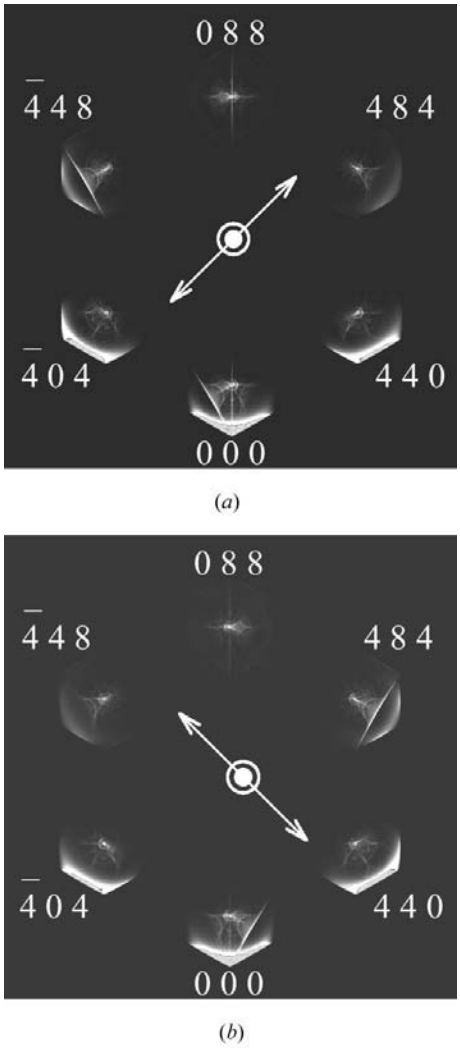

Figure 9
Photographs computer simulated by using the technique described in §3 assuming the six-beam case shown in this figure. White arrows approximately show the directions of polarization of the incident X-rays.

5. Conclusions

A real-space *n*-beam X-ray dynamical diffraction theory based on the Takagi–Taupin theory has been derived, where $n \in \{3, 4, 6, 8, 12\}$. The final equations (25) and (39) can be written in a simple form owing to the high symmetry of the equations. The difficulty of dealing with the effect of polarization has been overcome by dividing the electric displacement vectors into scalar components whose unit vectors cross obliquely. The derivation of the present theory is now opportune for the present age when X-ray phase retarders have been developed (Hirano *et al.*, 1991, 1992, 1993, 1995; Giles, Malgrange, Goulon, de Bergevin, Vettier, Dartyge *et al.*, 1994; Giles, Malgrange, Goulon, de Bergevin, Vettier, Fontaine *et al.*, 1994; Giles *et al.*, 1995) for obtaining an arbitrary polarization state of the X-rays with a high degree of polarization (Okitsu *et al.*, 2001, 2002). A computer program to solve the theory has been developed by the present author. The program is applicable for any *n*-beam case ($n \in \{3, 4, 6, 8, 12\}$) with several minor changes.

APPENDIX *A*
Consideration of the boundary condition for the incidence of plane-wave X-rays that deviate from the Bragg condition

The aim of the present paper is to give a simple form of Takagi–Taupin-type *n*-beam dynamical theory with a high symmetry so that the theory can be solved analytically or by using a computer. For this purpose, the Lorentz point is defined as described in (1)–(5). In Takagi's articles (Takagi, 1962, 1969), the starting point of wavevector $\mathbf{k}_i$ is not necessary at the Lorentz point; parameter β_i defines the deviation from this point. $\beta_i'(\mathbf{r})$ is defined by (7). However, even if β_i is zero, the generality of (6) does not collapse. Therefore, the final equations (25) and (39) are deduced from (8). Equation (39) can be solved even when plane-wave X-rays that deviate from the *n*-beam Bragg condition are incident on a crystal. The method to solve (39) in this case is described in the following paragraph.

Equation (39) is derived under the assumption that an X-ray wavefield $\mathbf{D}(\mathbf{r})$ is represented as in (27). To solve (39), a boundary condition $\mathbf{D}_0''(\mathbf{r}_e)$ has to be given so that the incidence condition of X-rays is correctly reflected on the solution of (39), where $\mathbf{r}_e$ is a location vector on the entrance surface of the crystal. Here, what is important for the generality of (39) derived with the wavevector $\mathbf{K}_i$ in (27) being fixed at $\overrightarrow{LaH_i}$ is that a boundary condition $\mathbf{D}_0''(\mathbf{r}_e)$ can properly be given when

the wavevector of the plane-wave X-rays deviates from $\overrightarrow{LaH_0}$. Now, let us consider a case where X-rays of electric displacement $\mathbf{D}_0^{\prime\prime(d)}$ and wavevector $\mathbf{K}_0^{(d)}$ are incident on the crystal. Wavefield $\mathbf{D}_0^{\prime\prime}(\mathbf{r})$ before the crystal is represented as follows:

$$\mathbf{D}_0^{\prime\prime}(\mathbf{r}) = \mathbf{D}_0^{\prime\prime(d)} \exp(-\mathrm{i}2\pi\mathbf{K}_0^{(d)} \cdot \mathbf{r}). \tag{41}$$

Here, considering that $\mathbf{K}_0^{(d)} = \mathbf{K}_0 - \Delta\mathbf{K}_0$, where $\Delta\mathbf{K}_0$ is a differential wavevector that depends on the angular deviation of the incident X-rays from the n-beam Bragg condition, (41) is transformed to

$$\mathbf{D}_0^{\prime\prime}(\mathbf{r}) = \mathbf{D}_0^{\prime\prime(d)} \exp(+\mathrm{i}2\pi\Delta\mathbf{K}_0 \cdot \mathbf{r}) \exp(-\mathrm{i}2\pi\mathbf{K}_0 \cdot \mathbf{r}). \tag{42}$$

Therefore, substituting $\mathbf{r}_e$ as $\mathbf{r}$ and comparing (42) with the term with $i = 0$ in (27), we obtain

$$\mathbf{D}_0^{\prime\prime}(\mathbf{r}_e) = \mathbf{D}_0^{\prime\prime(d)} \exp(+\mathrm{i}2\pi\Delta\mathbf{K}_0 \cdot \mathbf{r}_e). \tag{43}$$

Equation (43) is a boundary condition that should be given for the case that the incident plane-wave X-rays deviate from the n-beam Bragg condition. Takagi (1962, 1969) derived his fundamental equation in which parameters β_i were introduced to deal with the angular deviation of the incident X-rays from the Bragg condition. On the other hand, the present author has prepared a technique giving the boundary condition as is described in (43) and removed the parameter β_i from the fundamental equation in order to obtain highly symmetrical forms of the final equations (25) and (39). In the usual procedure using the dispersion surfaces derived in the Ewald–Laue two-beam theory, four tie points (two each for σ and π polarizations) are excited along a crystal-surface normal drawn inward from the starting point of the wavevector of the incident X-rays. This treatment is only based on the condition of continuity of the wavefront between inside and outside the crystal surface, which is naturally satisfied in the boundary condition described as (43). The traditional procedure using the inward drawn normal and the dispersion surfaces can only deal with a case that the crystal surfaces are planar. On the other hand, the boundary condition described as (43) is more general since it can even deal with the case that the crystal surfaces are not planar.

APPENDIX *B*
Validity of scalar displacements with unit vector crossing obliquely to which the electric displacement vectors are expanded

In §2.5, the electric displacement vectors are expanded to the combination of scalar values as in (16). Unit vectors $\mathbf{e}_i$ and $\mathbf{e}_{(i+1)'}$ cross obliquely. In §2.5, (22) is considered to be evident. Here, let us verify (22) by using the unit vectors $\mathbf{s}_i$, $\mathbf{e}_i^{(\sigma)}$ and $\mathbf{e}_i^{(\pi)}$ which construct an orthogonal coordinate system defined by (19) and (20). $\mathbf{D}_i(\mathbf{r})$ can be represented as follows:

$$\mathbf{D}_i(\mathbf{r}) = D_i^{(\sigma)}(\mathbf{r})\mathbf{e}_i^{(\sigma)} + D_i^{(\pi)}(\mathbf{r})\mathbf{e}_i^{(\pi)}. \tag{44}$$

We obtain the following relations by referring to Fig. 6:

$$\mathbf{e}_i = -\cos\alpha_i\mathbf{e}_i^{(\sigma)} + \sin\alpha_i\mathbf{e}_i^{(\pi)}, \tag{45}$$

$$\mathbf{e}_{(i+1)'} = \cos\alpha_i\mathbf{e}_i^{(\sigma)} + \sin\alpha_i\mathbf{e}_i^{(\pi)}. \tag{46}$$

Then, we also obtain the following relations by referring to Fig. 6:

$$\mathbf{e}_i^{(\sigma)} = -\frac{1}{2\cos\alpha_i}\mathbf{e}_i + \frac{1}{2\cos\alpha_i}\mathbf{e}_{(i+1)'}, \tag{47}$$

$$\mathbf{e}_i^{(\pi)} = \frac{1}{2\sin\alpha_i}\mathbf{e}_i + \frac{1}{2\sin\alpha_i}\mathbf{e}_{(i+1)'}. \tag{48}$$

Substituting (45) and (46) into (16), we find

$$\begin{aligned}\mathbf{D}_i(\mathbf{r}) = {} & [-\cos\alpha_i D_i^{(0)}(\mathbf{r}) + \cos\alpha_i D_i^{(1)}(\mathbf{r})]\mathbf{e}_i^{(\sigma)} \\ & + [\sin\alpha_i D_i^{(0)}(\mathbf{r}) + \sin\alpha_i D_i^{(1)}(\mathbf{r})]\mathbf{e}_i^{(\pi)}.\end{aligned} \tag{49}$$

Comparing (44) and (49), we obtain

$$D_i^{(\sigma)}(\mathbf{r}) = -\cos\alpha_i D_i^{(0)}(\mathbf{r}) + \cos\alpha_i D_i^{(1)}(\mathbf{r}), \tag{50}$$

$$D_i^{(\pi)}(\mathbf{r}) = \sin\alpha_i D_i^{(0)}(\mathbf{r}) + \sin\alpha_i D_i^{(1)}(\mathbf{r}). \tag{51}$$

In the case using the orthogonal coordinate system, the following relation is evident:

$$\begin{aligned}(\mathbf{s}_i \cdot \mathrm{grad})\mathbf{D}_i(\mathbf{r}) &= \frac{\partial}{\partial s_i}\mathbf{D}_i(\mathbf{r}) \\ &= \frac{\partial}{\partial s_i}D_i^{(\sigma)}\mathbf{e}_i^{(\sigma)} + \frac{\partial}{\partial s_i}D_i^{(\pi)}\mathbf{e}_i^{(\pi)}.\end{aligned} \tag{52}$$

Substituting (47), (48), (50) and (51) into (52), we get

$$\begin{aligned}&(\mathbf{s}_i \cdot \mathrm{grad})\mathbf{D}_i(\mathbf{r}) \\ &= \frac{\partial}{\partial s_i}[-\cos\alpha_i D_i^{(0)}(\mathbf{r}) + \cos\alpha_i D_i^{(1)}(\mathbf{r})] \\ &\quad \times \left(-\frac{1}{2\cos\alpha_i}\mathbf{e}_i + \frac{1}{2\cos\alpha_i}\mathbf{e}_{(i+1)'}\right) \\ &\quad + \frac{\partial}{\partial s_i}[\sin\alpha_i D_i^{(0)}(\mathbf{r}) + \sin\alpha_i D_i^{(1)}(\mathbf{r})] \\ &\quad \times \left(\frac{1}{2\sin\alpha_i}\mathbf{e}_i + \frac{1}{2\sin\alpha_i}\mathbf{e}_{(i+1)'}\right) \\ &= \frac{\partial}{\partial s_i}[\tfrac{1}{2}D_i^{(0)}(\mathbf{r}) - \tfrac{1}{2}D_i^{(1)}(\mathbf{r}) + \tfrac{1}{2}D_i^{(0)}(\mathbf{r}) + \tfrac{1}{2}D_i^{(1)}(\mathbf{r})]\mathbf{e}_i \\ &\quad + \frac{\partial}{\partial s_i}[-\tfrac{1}{2}D_i^{(0)}(\mathbf{r}) + \tfrac{1}{2}D_i^{(1)}(\mathbf{r}) + \tfrac{1}{2}D_i^{(0)}(\mathbf{r}) + \tfrac{1}{2}D_i^{(1)}(\mathbf{r})]\mathbf{e}_{(i+1)'} \\ &= \frac{\partial}{\partial s_i}D_i^{(0)}(\mathbf{r})\mathbf{e}_i + \frac{\partial}{\partial s_i}D_i^{(1)}(\mathbf{r})\mathbf{e}_{(i+1)'}\end{aligned} \tag{53}$$

Equation (53) verifies the relation (22).

The present work was performed at the High-Power X-ray Laboratory, School of Engineering, The University of Tokyo, and is one of the activities of the Active Nano-Characterization and Technology Project financially supported by Special Coordination Funds of the Ministry of Education, Culture, Sports, Science and Technology of the Japan Government. This paper is dedicated to Professor Norio Kato who passed away 5 April 2002.

References

Authier, A. (2001). *Dynamical Theory of X-ray Diffraction.* Oxford University Press.
Authier, A. & Malgrange, C. (1998). *Acta Cryst.* A**54**, 806–819.
Balibar, F. & Authier, A. (1967). *Phys. Status Solidi*, **21**, 413–422.
Berg, O. (1926). *Naturwissenschaften*, **14**, 886–887.
Bijvoet, J. M. & MacGillavry, C. H. (1939). *Chem. Weekbl.* **36**, 330–331.
Blanc, M. & Weigle, J. (1937). *Helv. Phys. Acta*, **10**, 495–506.
Burbank, R. D. (1965). *Acta Cryst.* **19**, 957–962.
Cauchois, Y., Hulubei, H. & Weigle, J. (1937). *Helv. Phys. Acta*, **10**, 218–224.
Chang, S. L. (1986). *Phys. Rev. B*, **33**, 5848–5850.
Colella, R. (1974). *Acta Cryst.* A**30**, 413–423.
Darwin, C. G. (1914*a*). *Philos. Mag.* **27**, 315–333.
Darwin, C. G. (1914*b*). *Philos. Mag.* **27**, 675–690.
Epelboin, Y. (1985). *Mater. Sci. Eng.* **73**, 1–43.
Epelboin, Y. (1987). *Prog. Cryst. Growth Charact.* **14**, 465–506.
Ewald, P. P. (1917). *Ann. Phys. (Leipzig) 4. Folge*, **54**, 519–597.
Ewald, P. P. & Héno, Y. (1968). *Acta Cryst.* A**24**, 5–15.
Giles, C., Malgrange, C., Goulon, J., de Bergevin, F., Vettier, C., Dartyge, E., Fontaine, A., Giorgetti, C. & Pizzini, S. (1994). *J. Appl. Cryst.* **27**, 232–240.
Giles, C., Malgrange, C., Goulon, J., de Bergevin, F., Vettier, C., Fontaine, A., Dartyge, E. & Pizzini, S. (1994). *Nucl. Instrum. Methods A*, **349**, 622–625.
Giles, C., Vettier, C., de Bergevin, F., Malgrange, C., Grübel, G. & Grossi, F. (1995). *Rev. Sci. Instrum.* **66**, 1518–1521.
Green, G. S., Fan, C.-S. & Tanner, B. K. (1990). *Philos. Mag. A*, **61**, 23–33.
Härtwig, J. (2001). *J. Phys. D*, **34**, A70–A77.
Hirano, K., Ishikawa, T. & Kikuta, S. (1993). *Nucl. Instrum. Methods Phys. Res. A*, **336**, 343–353.
Hirano, K., Ishikawa, T. & Kikuta, S. (1995). *Rev. Sci. Instrum.* **66**, 1604–1609.
Hirano, K., Ishikawa, T., Koreeda, S., Fuchigami, K., Kanzaki, K. & Kikuta, S. (1992). *Jpn. J. Appl. Phys.* **31**, L1209–L1211.
Hirano, K., Izumi, K., Ishikawa, T., Annaka, S. & Kikuta, S. (1991). *Jpn. J. Appl. Phys.* **30**, L407–L410.
Kato, N. (1961*a*). *Acta Cryst.* **14**, 526–532.
Kato, N. (1961*b*). *Acta Cryst.* **14**, 627–636.
Kato, N. (1968*a*). *J. Appl. Phys.* **39**, 2225–2230.
Kato, N. (1968*b*). *J. Appl. Phys.* **39**, 2231–2237.
Kato, N. (1976*a*). *Acta Cryst.* A**32**, 453–457.
Kato, N. (1976*b*). *Acta Cryst.* A**32**, 458–466.
Kato, N. (1979). *Acta Cryst.* A**35**, 9–16.
Kato, N. (1980*a*). *Acta Cryst.* A**36**, 171–177.
Kato, N. (1980*b*). *Acta Cryst.* A**36**, 763–769.
Kato, N. (1980*c*). *Acta Cryst.* A**36**, 770–778.
Larsen, H. B. & Thorkildsen, G. (1998). *Acta Cryst.* A**54**, 137–145.
Laue, M. von (1931). *Ergeb. Exakten Naturwiss*, **10**, 133–158.
Lipscomb, W. N. (1949). *Acta Cryst.* **2**, 193–194.
Mayer, G. (1928). *Z. Kristallogr.* **66**, 585–636.
Okitsu, K. (2003). *Acta Cryst.* A. In preparation.
Okitsu, K., Iida, S., Sugita, Y., Takeno, H., Yagou, Y. & Kawata, H. (1992). *Jpn. J. Appl. Phys*, **31**, 3779–3785.
Okitsu, K., Imai, Y., Ueji, Y. & Yoda, Y. (2003). *Acta Cryst.* A. Submitted.
Okitsu, K., Ueji, Y., Sato, K. & Amemiya, Y. (2001). *J. Synchrotron Rad.* **8**, 33–37.
Okitsu, K., Ueji, Y., Sato, K. & Amemiya, Y. (2002). *Acta Cryst.* A**58**, 146–154.
Ott, H. (1938). *Ann. Phys. (Leipzig) 5. Folge*, **31**, 264–288.
Post, B. (1977). *Phys. Rev. Lett.* **39**, 760–763.
Post, B. (1979). *Acta Cryst.* A**35**, 17–21.
Renninger, M. (1937). *Z. Phys.* **106**, 141–176.
Schachenmeier, R. (1923). *Z. Phys.* **19**, 94–111.
Shen, Q. (1986). *Acta Cryst.* A**42**, 525–533.
Stetsko, Y. P., Juretschke, H. J., Huang, Y.-S., Lee, Y.-R., Lin, T.-C. & Chang, S.-L. (2001). *Acta Cryst.* A**57**, 359–367.
Takagi, S. (1962). *Acta Cryst.* **15**, 1311–1312.
Takagi, S. (1969). *J. Phys. Soc. Jpn*, **26**, 1239–1253.
Taupin, D. (1964). *Bull. Soc. Fr. Minéral. Cristallogr.* **87**, 469–511.
Taupin, D. (1967). *Acta Cryst.* **23**, 25–35.
Thorkildsen, G. (1987). *Acta Cryst.* A**43**, 361–369.
Thorkildsen, G. & Larsen, H. B. (1998). *Acta Cryst.* A**54**, 120–128.
Thorkildsen, G., Larsen, H. B. & Weckert, E. (2001). *Acta Cryst.* A**57**, 389–394.
Wagner, E. (1920). *Phys. Z.* **21**, 621–626.
Weckert, E. & Hümmer, K. (1997). *Acta Cryst.* A**53**, 108–143.
Weckert, E. & Hümmer, K. (1998). *Cryst. Res. Technol.* **33**, 653–678.
Weckert, E., Schwegle, W. & Hümmer, K. (1993). *Proc. R. Soc. London Ser. A*, **442**, 33–46.
Weigle, J. & Mühsam, H. (1937). *Helv. Phys. Acta*, **10**, 139–156.